




# Polyethylene glycol–gum acacia-based multidrug delivery system for controlled delivery of anticancer drugs

V. O. Fasiku<sup>1</sup> · B. A. Aderibigbe<sup>2</sup>  · E. R. Sadiku<sup>3</sup> · Y. Lemmer<sup>4</sup> · S. J. Owonubi<sup>1,7</sup> · S. S. Ray<sup>5,6</sup> · E. Mukwevho<sup>1</sup>

Received: 6 April 2018 / Revised: 20 November 2018 / Accepted: 28 November 2018 /  
Published online: 6 December 2018  
© Springer-Verlag GmbH Germany, part of Springer Nature 2018

## Abstract

Breast cancer is a chronic disease that is characterized by an uncontrolled growth of abnormal cells from the breast tissue. It is one of the leading causes of mortality among women worldwide because of its early metastasis, aggressive behavior and resistance to the currently used anticancer drugs. Most of these drugs suffer from poor absorption and toxicity, and lack long-term efficaciousness because of drug resistance. Recently, polymeric thermosensitive hydrogels have emerged as excellent drug delivery systems for anticancer drugs with the potential to improve the overall therapeutic effect of the incorporated drug. In this current research, doxorubicin and curcumin were loaded into biodegradable PEG–gum acacia-based hydrogels. These hydrogels were pH-sensitive, biodegradable and non-toxic. The release mechanism of the drugs from the hydrogels was pH-dependent. In vitro cytotoxicity studies on MCF-7 cancer cell lines further confirmed that the incorporation of doxorubicin and curcumin into the hydrogels resulted in significant cytotoxic effect when compared

✉ B. A. Aderibigbe  
blessingaderibigbe@gmail.com

✉ E. Mukwevho  
emmanuel.mukwevho@nwu.ac.za

<sup>1</sup> Department of Biological Science, North-West University, Private Bag X2046, Mmabatho 2735, South Africa

<sup>2</sup> Department of Chemistry, University of Fort Hare, Alice Campus, Alice, Eastern Cape, South Africa

<sup>3</sup> Institute of Nano Engineering Research (INER) and Department of Chemical, Metallurgical and Materials Engineering, Tshwane University of Technology, Pretoria, South Africa

<sup>4</sup> CSIR Biosciences, CSIR, Pretoria 0001, South Africa

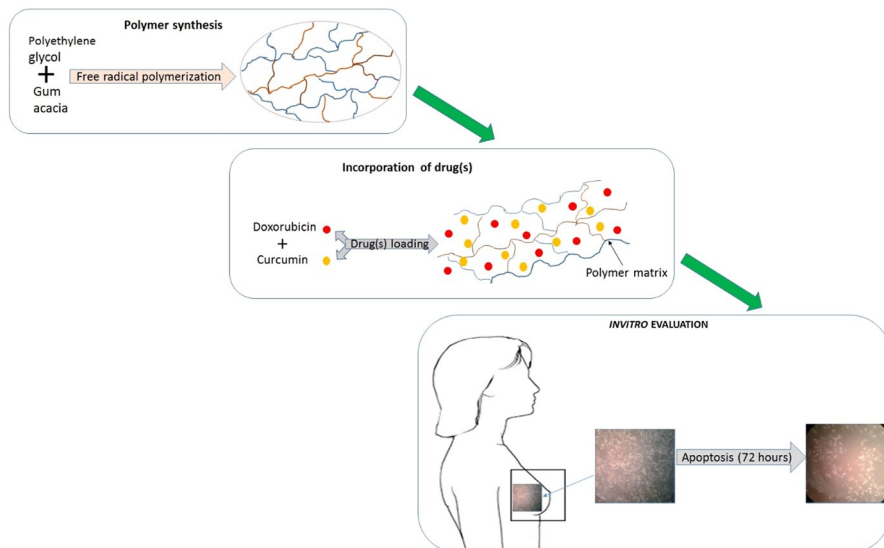
<sup>5</sup> DST/CSIR National Centre for Nanostructured Materials, Council for Scientific and Industrial Research, Pretoria 0001, South Africa

<sup>6</sup> Department of Applied Chemistry, University of Johannesburg, Doornfontein, Johannesburg 2028, South Africa

<sup>7</sup> Department of Chemistry, University of Zululand, KwaDlangezwa, KwaZulu-Natal, South Africa

to the free drugs, suggesting that these hydrogels are potential dual-drug delivery systems. The cytotoxic effect was dose- and time-dependent.

### Graphical abstract



**Keywords** Breast cancer · Hydrogel · Dual-drug delivery systems · Curcumin · Doxorubicin

### Introduction

Breast cancer has been identified as one of the leading causes of deaths among all types of cancers all over the world. Thus, it has become a serious public health issue [1]. It is the most frequently diagnosed disease among women. Therefore, there is a pressing need to employ non-surgical therapies for its treatment and management. At the moment, a number of chemotherapeutic agents are used, but there are some challenges faced with the use of these chemotherapeutics, such as drug resistance, poor water solubility, lack of cell specificity and drug toxicity [2]. Cancer cells have become resistant to several drugs used in the management of the disease and this has led to the application of combination therapy. This is evident in a report by Asghar and his colleague where they reviewed past and current causes of drug resistance by cancerous cells. They also suggested strategies by which the barrier can be overcome [3].

Combination therapy which involves combining two or more therapeutic agents for the treatment of breast cancer has resulted in improved long-term prognosis over the years. This is achieved by targeting different pathways by the drugs. The

advantages of combination therapy approach include: reduced side effects and ability to overcome drug resistance and the therapeutic effect of the drug is maximized. This was demonstrated in an experiment by Saraswathy and her co-workers by using two anticancer agents in a targeted drug delivery system [4, 5]. Doxorubicin and curcumin are examples of potential therapeutic drugs for combination therapy. Doxorubicin belongs to the anthracycline antibiotic family. It is one of the drugs with great efficacy in the treatment of breast cancer. However, its clinical application has been greatly limited because of toxicity such as cardiotoxicity [6]. Curcumin, on the other hand, is a polyphenol from *Curcuma longa*, a perennial herb. It has antioxidant, antiangiogenic, anti-inflammatory, antimicrobial and anticancer activities [7]. However, it is not soluble in water with poor bioavailability which limits its clinical use [8].

The mode of action of curcumin as an anticancer drug is by the inhibition the STAT3 and NF- $\kappa$ B pathways, which play key roles in breast cancer development and progression; inhibition of cell proliferation, cell cycle arrest and stimulation of apoptosis via modulation of other transcription factors, such as AP-1,  $\beta$ -catenin, Erg-1, Notch-1, p53, Hif-1; and PPAR- $\alpha$  down-regulation of Sp-1, a transcription factor which is highly expressed in breast cancer and reverses multidrug resistance [9–11]. On the other hand, doxorubicin mode of action on cancer cell is by intercalation into the DNA and disruption of topoisomerase-II-mediated DNA repair and by the generation of free radicals and their damage to DNA, cellular membranes and proteins [12, 13]. Due to the different mode of action of curcumin and doxorubicin, the combination of both drugs has been studied using selected polymer-based drug delivery systems such as micelles, liposomes and nanoparticles, resulting in synergistic effects.

Polymeric hydrogels are polymer-based drug delivery systems, which have been reported to be effective in the management of several diseases such as cancer, due to their ability to accumulate therapeutic agents at specific sites [14]. Hydrogels are non-toxic, biocompatible, biodegradable, porous, and have good swelling properties and tunable mechanical properties; depending on their application, they can be tailored to respond to stimuli such as temperature and pH [15, 16]. There are several synthetic and natural polymers, which have been explored for the design of hydrogels such as chitosan, polyethylene glycol (PEG), sodium alginate and gum acacia. The application of PEG and gum acacia for the design of hydrogels for drug delivery has been reported by some researchers, resulting in systems which are temperature- and pH-sensitive, non-toxic, biodegradable, hydrophilic, non-immunogenic with controlled drug release mechanism and suitable for dual-drug delivery systems [17–20]. PEG-based hydrogel drug release profile can be tuned by changing the hydrophobicity effect of the gels. Giray et al. [21] demonstrated the controlled drug delivery capability of PEG hydrogels. In addition, PEG-based hydrogel has been reported to be temperature-sensitive and biodegradable with sustained drug release profile [22]. Hydrogels containing gum acacia have also been reported by some researchers to be non-toxic, biodegradable with a good swelling capability and suitable for controlled drug delivery [23–25]. Despite all these studies on hydrogels, there is still no report on hydrogels containing PEG and gum acacia developed for the delivery of anticancer drugs.

The only report on hydrogel loaded with both drugs was reported by Cao et al. in which doxorubicin and curcumin were loaded into a thixotropic injectable silk fibroin/hydroxypropyl cellulose hydrogels for localized chemotherapy of solid tumor. In vitro and in vivo studies revealed sustained and enhanced antitumor efficacy which was very significant when compared with the free drug or single drug-loaded hydrogels [26]. Other polymer-based drug delivery systems have also been investigated for the delivery of the combination DOX and curcumin, resulting in a synergistic effect. Barui et al. loaded curcumin and doxorubicin PEGylated liposomes, resulting in enhanced tumor growth inhibition which was two- to threefold more than mice treated with formulations containing only curcumin or doxorubicin in vivo [27]. Zhao et al. loaded curcumin and DOX into nanoparticles which revealed curcumin capability to reverse multidrug resistance which was significant by the reduced mRNA levels of *MDR1*, *bcl-2* and *HIF-1 $\alpha$* , and protein levels of P-gp, Bcl-2 and HIF-1 $\alpha$ . A significant cytotoxic effect, decreased IC<sub>50</sub> and resistant index further confirmed the synergistic effects of combining both drugs [28]. Zhang et al. [29] confirmed similar findings in which polymer-based nanoparticles loaded with both drugs prolonged blood circulation time, elevated drug accumulation with increased tumor inhibitory effect when compared to the free drugs.

Based on the findings from other researchers using different systems, the aim of this study is to evaluate the potential of a PEG-based hydrogel as a dual-drug delivery system for combination therapy. In this study, a PEG-based hydrogel was synthesized by a free radical polymerization reaction. The resultant hydrogel was characterized by using Fourier transform infrared (FTIR), scanning electron microscope (SEM), X-ray diffraction (XRD), thermogravimetric analysis (TGA), and followed by an in vitro cytotoxicity assay of drug-loaded hydrogel on MCF-7 breast cancer cell lines in order to evaluate its potential as a drug delivery system for combination therapy.

## Materials and methods

### Materials

All reagents used were analytical grade and they were purchased from Merck Chemicals (South Africa): *N,N*-methylenebisacrylamide (MBA), gum acacia, acrylic acid, *N,N,N,N*-tetramethylethylenediamine (TEMED), potassium persulfate (KPS), polyethylene glycol 4000 (MW 3600–4400 g/mol) (PEG), acrylamide, *N*-isopropylacrylamide (NIPAM) and the cell culture reagents were supplied by Merck Chemicals (South Africa). Curcumin and doxorubicin were also supplied by Merck Chemicals (Darmstadt, Germany), while MCF-7 cell lines were purchased from Cellonex cell line, LOT: 01.

### Synthesis of PEG-based hydrogel

The PEG-based hydrogel was prepared by a modified procedure reported by Varaprasad et al. [30]. 0.05 g of gum acacia was dissolved in 2 mL of 6.49 mM MBA followed by

continuous stirring. 1 g of acrylamide, 0.5 g of PEG, 0.5 g of acrylic acid, 1% *N*-isopropylacrylamide, 36.7 mM KPS and 86 mM TEMED were added, respectively. The resultant solution was left to polymerize at a temperature of 40–60 °C, resulting in the formation of a gel which was soaked in distilled water overnight in order to remove unreacted reagents. The resulting gel was dried at ambient temperature for 5 days.

### Loading of doxorubicin and curcumin into the hydrogel

Doxorubicin (DOX.HCl) and curcumin (5 mg each) were dissolved in appropriate solvents, and they were subsequently loaded unto 100 mg of the synthesized hydrogel. The two drugs (2.5 mg each) were loaded in combination into 100 mg of the hydrogel. This was done according to the procedure of Varaprasad et al. [30]. The hydrogels were rinsed with distilled water thoroughly in order to get rid of excess drug (DOX.HCl) and curcumin on the surface of the hydrogels, and dried for 5 days at ambient temperature. It is important to mention that curcumin is hydrophobic in nature when compared to doxorubicin salt which is hydrophilic in nature. The percentage drug entrapment efficiency was calculated according to Eq. (1):

$$\% \text{ Drug entrapment efficiency} = \frac{\text{Actual drug loading (mg)}}{\text{Theoretical drug loading (mg)}} \times 100 \quad (1)$$

### Swelling studies

The swelling capacity of the PEG-based hydrogel was investigated using a gravimetric method to measure the equilibrium swelling behavior of the hydrogel [31]. About 0.3 g of the PEG-based hydrogel was placed in beakers containing varying pHs (1.2, 5.8 and 7.4) of about 25 mL and allowed to swell at room temperature. At an interval of 30 min (over a period of 6 h), the hydrogel was blotted with a filter paper (in order to get rid of excess solutions on the surface), weighed on an electronic weighing balance and returned into the buffers. Subsequently, it was weighed at 12, 24, 48 and 72 h, respectively. The swelling ratio and equilibrium swelling ratio of the hydrogel were calculated gravimetrically using the equations as follows:

#### Equilibrium swelling ratio:

$$S_r = \left( \frac{W_t - W_o}{W_o} \right) \quad (2)$$

$$S_{\text{eq}} = \left( \frac{W_s - W_t}{W_s} \right) \quad (3)$$

$$S\% = \left( \frac{W_t - W_o}{W_o} \right) \times 100 \quad (4)$$

where  $S_t$  = swelling ratio (g/g);  $W_t$  = weight at time  $t$  (g);  $W_0$  = initial weight of the hydrogel before swelling (g);  $W_s$  = swollen hydrogel weight (g);  $S\%$  = percentage water uptake of the hydrogels;  $S_{eq}$  = equilibrium swelling ratio (g/g).

The solvent diffusion and polymer matrix relaxation effect were calculated and analyzed by examining the exponent  $n$  from Eq. 5.

$$\frac{W_t}{W_\infty} = Kt^n \quad (5)$$

where  $W_t$  = weight of hydrogel (g) at time,  $t$ ;  $W_\infty$  = weight of hydrogel at equilibrium (g);  $K$  = diffusion constant;  $n$  = diffusion exponent.

The diffusion exponent  $n$  was determined from the slope of the graph of  $\ln(W_t/W_\infty)$  versus  $\ln(t)$ .

The diffusion coefficient was calculated using Eq. (6):

$$S = 4 \left[ \frac{D}{\pi r^2} \right]^{\frac{1}{2}} \cdot t^{\frac{1}{2}} \quad (6)$$

where  $D$  = diffusion coefficient of the hydrogel;  $r$  = radius of the hydrogel;  $S$  = fractional swelling;  $t$  = time.

The diffusion coefficients were evaluated from the plot of  $S$  versus  $t^{1/2}$  and these were obtained from the slopes.

## Characterization

### Fourier transform infrared (FTIR)

The hydrogel sample [with and without the drug(s)] was analyzed using a PerkinElmer Spectrum 100 FTIR spectrometer. This was done in the wavelength range between 4000 and 500  $\text{cm}^{-1}$ . Sixteen scans were used at a resolution of 4  $\text{cm}^{-1}$ . The background was scanned to act as a control before the sample was analyzed.

### X-ray diffraction (XRD)

In order to identify the interaction of the drug(s) within the hydrogel, X-ray diffraction was employed using a PANalytical X'Pert PRO diffractometer ( $\text{CuK}_\alpha$  radiation, with a wavelength,  $\lambda = 0.1546$  nm) running at 40 kV and 40 mA. The XRD technique was performed in order to evaluate and understand the morphological changes in the structure and crystallinity of the sample.

### Scanning electron microscope (SEM)

The sample was mounted on a carbon tape and then coated with gold. Thereafter, the sample was put into a Jeol JSM-5600 SEM for analysis. Images were formed at different magnification after appropriate focusing was done.

## Thermogravimetric analysis (TGA)

The sample was placed into the analyzer of a TA TGA Q500 machine, ensuring that there was no moisture on the plate in order to have accurate results. The sample was analyzed at a heating rate of 10 °C per minute, under air and ramped up to 900 °C. The plot of the weight loss was done on the data obtained from the result of the analysis.

## UV–visible spectrophotometer

The amount of drug released from the hydrogels was determined using a Cary 100 UV–visible instrument. Prior to the analysis, the spectrophotometer was switched on for 20 min to allow sufficient heating up time. The wavelength used for the analysis was dependent on the wavelength of the drug loaded into the hydrogel. Before recording the absorbance of the samples, autozero and standards were performed to ensure accurate results are obtained.

## Release studies

Buffer solutions at pH 1.2, 5.8 and 7.4 were prepared and placed in a water bath shaker—BS-06 Lab Companion (set at 37 °C)—overnight to equilibrate. The hydrogel loaded with the drugs was placed in 3 mL of the equilibrated buffers. The water bath was set to 50 rpm at 37 °C, and at 30-min interval (for 6 h), the entire buffer was removed and then stored. The exact quantity of the buffer that was removed was then replaced. This was also done subsequently at 24, 48 and 72 h, respectively. In order to determine the drug release concentrations at different time intervals, the stored buffer solutions were analyzed using a UV spectrophotometer. The amounts of curcumin and doxorubicin released were measured at 427 nm and 480 nm, respectively. Drug release kinetics was performed as reported by Aderibigbe et al. [32]. Percentage cumulative drug release was calculated as:

$$\left(\frac{I_o}{I_f}\right) \times 100 \quad (7)$$

where  $I_o$  = initial amount of drug released (mg) at time  $t$ ;  $I_f$  = total amount of drug loaded into the hydrogel (mg).

Using the percentage of cumulative release data obtained from Eq. 7, different drug release kinetic models were employed in this study:

## Korsmeyer–Peppas:

$$\left(\frac{M_t}{M_\infty}\right) = Kt^n \quad (8)$$

where  $\frac{M_t}{M_\infty}$  = fraction of drug released;  $K$  = release constant;  $n$  = release exponent;  $t$  = time of release.

### Zero-order:

$$C = C_0 - K_0^t \quad (9)$$

where  $C$  = amount of dissolved or released drug (mg);  $C_0$  = initial amount of drug in solution (mg);  $K_0$  = zero-order rate constant;  $t$  = time.

### Hixson–Crowell:

$$C_0^{\frac{1}{3}} - C_t^{\frac{1}{3}} = K_{HC} t \quad (10)$$

where  $C_t$  = amount of drug released (mg) at time  $t$ ;  $C_0$  = initial amount of drug (mg);  $K_{HC}$  = Hixson–Crowell's rate constant.

### Higuchi:

$$C = [D(2qt - C_s)C_s t]^{\frac{1}{2}} \quad (11)$$

where  $C$  = total amount of released drug per unit area of the matrix (mg);  $D$  = diffusion coefficient for the drug in the matrix;  $qt$  = total amount of the drug in a unit volume of the matrix (mg);  $C_s$  = dimensional solubility of the drug in the polymer matrix;  $t$  = time (h).

## In vitro cytotoxicity studies

The cytotoxicity of hydrogel [loaded and unloaded with the drug(s)] was evaluated by WST assay on MCF-7 breast cancer cell lines in order to determine the cell toxicity. The WST assay is a colorimetric cell proliferation assessment, based on the tetrazolium salt (WST-1) which is reduced to water-soluble orange formazan by cellular mitochondrial dehydrogenase present in viable cells. Therefore, the quantity of formazan dye, determined by the absorbance at 450 nm, is directly proportional to the number of living cells. The cells ( $1 \times 10^5$  cells/mL) were seeded into 96-well plates in complete media without antibiotics for 48 h and then treated with 0.055–28  $\mu\text{g/mL}$  of the drug(s). Untreated cells were used as the control. 10  $\mu\text{L}$  of WST was added to each well, and the plate was incubated for 1 h 30 min. The absorbance was measured using a microtiter plate reader (Infinite<sup>®</sup> 200 PRO; Tecan Group Ltd., CSIR, South Africa) at the wavelength of 450 nm, and an individual experiment was carried out three times. The minimum inhibitory concentration (IC<sub>50</sub>) value was determined using GraphPad Prism software version 6.0 (GraphPad Software, Inc., La Jolla, CA, USA).



## Drug loading of hydrogels for in vitro cytotoxicity evaluation

5 mg of drug was weighed, dissolved in 1 mL of distilled water and mixed thoroughly using a vortex. The required concentration was pipetted from the stock concentration using a micropipette. The required concentration of drugs 0.055–28  $\mu\text{g}/\text{mL}$  was prepared. 1 mL aliquot of the required concentration was transferred into a 2-mL Eppendorf tube, and 21–24 mg hydrogel was inserted and allowed to imbibe the solution and then dried at room temperature before in vitro cytotoxicity evaluation.

## Statistical analysis

One-way analysis of variance was used to determine statistical significance. The results are expressed as mean  $\pm$  the standard error of the mean.  $p$  values  $< 0.05$  were considered statistically significant. The statistical analysis was performed using GraphPad Prism software version 6.0 (GraphPad Software, Inc., La Jolla, CA, USA).

## Results

### Swelling studies

The swelling studies of the hydrogel were carried out in buffers of 1.2, 5.8 and 7.4 in order to mimic the gastrointestinal tract, tumor cells and intestinal fluid—blood—respectively, at room temperature. The swelling capacity of the hydrogels was pH- and temperature-dependent. The hydrogel exhibited low swelling in the medium of pH 1.2 and 5.8, and a high swelling at pH 7.4 (Fig. 1a, b). The degree of swelling of the hydrogel increased with time until equilibrium swelling was reached. The swelling ratio (g/g) of the hydrogel at room temperature was 6, 11 and 22 at pH 1.2, 5.8 and 7.4, respectively. At 37 °C, the swelling ratio was 8, 14 and 28 g/g at pH 1.2, 5.8 and 7.4, respectively.

Table 1 indicates the swelling exponent ( $n$ ), the coefficient of correlation ( $R^2$  values) and the constant  $k$  as determined by the plot of the graph  $\text{Ln}(M_t/M_\infty)$  against  $\text{Ln } t$ . Results obtained indicated that the solvent diffusion was Fickian in the buffer of pH 1.2 and non-Fickian (anomalous) in the buffers of pH 5.8 and 7.4 since  $n$  values are  $> 0.5$  and  $0.5 < n < 1.00$ , respectively, at room temperature. At 37 °C, swelling exponents were 0.424, 0.290 and 0.523 at pH 1.2, 5.8 and 7.4, respectively, revealing pseudo-Fickian at pH 1.2, 5.8 and anomalous at pH 7.4. An excellent linearity was seen in all buffers with  $R^2$  values of 0.98–0.99. Similarly, the slope of the graph of swelling ratio against  $t^{1/2}$ , which represent the diffusion coefficient ( $D$ ) of the hydrogel for 50% of the total water uptake was determined. The diffusion coefficient of the hydrogels at room temperature was 0.824 at pH 7.4 when compared to 0.423 at pH 5.8 and 0.204 at pH 1.2, indicating

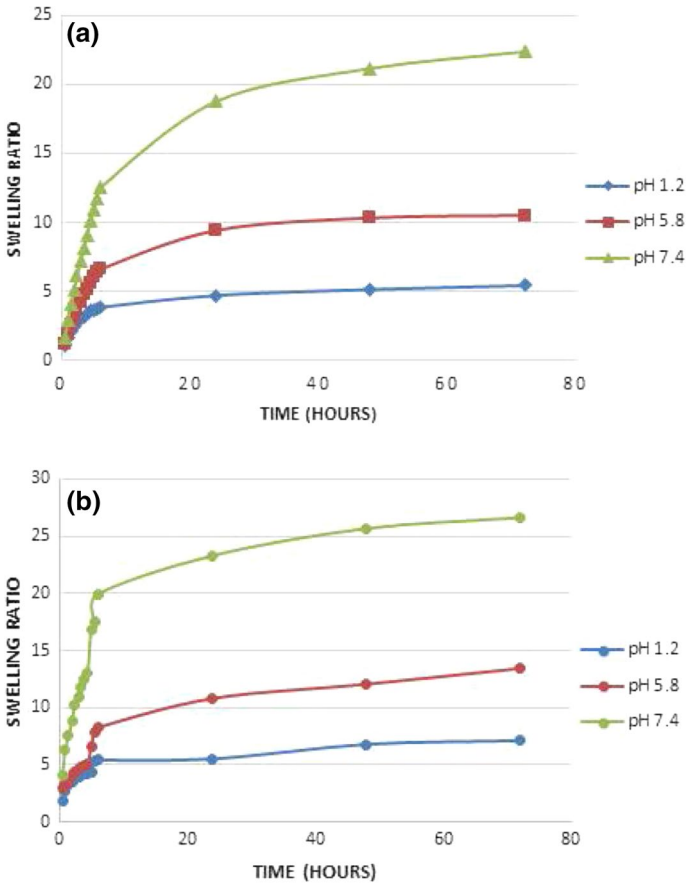


**Fig. 1** **a** A graph of swelling of hydrogels at room temperature. **b** A graph of swelling of hydrogels at 37 °C

**Table 1** Swelling data of the hydrogel at pH 1.2, 5.8 and 7.4 (a) at room temperature, (b) at 37 °C temperature

pH	$R^2$ (graph of $\ell n$ SR vs $\ell n$ time)	$n$	$k$	$R^2$ (graph of SR vs. $t^{1/2}$ )	$n$	$k$
<b>(a) At room temperature</b>						
1.2	0.99	0.504	1.56	0.99	0.204	1.14
5.8	0.99	0.716	2.29	0.99	0.423	1.39
7.4	0.99	0.814	2.25	0.99	0.824	3.52
<b>(b) At 37 °C temperature</b>						
1.2	0.979	0.424	0.80	0.985	0.296	1.27
5.8	0.982	0.290	0.29	0.976	0.215	1.62
7.4	0.991	0.523	0.38	0.995	0.827	2.60

faster diffusion at pH 7.4. At 37 °C, the diffusion coefficient was 0.296, 0.215 and 0.827 at pH 1.2, 5.8 and 7.4, respectively.

## Release studies

The percentage cumulative release of the drug(s) over a period of 72 h at different pH is shown in Table 2. The release of the drug from the hydrogels loaded with a single drug was enhanced when compared to hydrogels loaded with both drugs. 79%, 68% and 62% of doxorubicin were released from the hydrogel loaded with only doxorubicin at pH 1.2, 5.8 and 7.4, respectively. The release of curcumin from the hydrogel was 42%, 91% and 72% at pH 1.2, 5.8 and 7.4, respectively. The release of curcumin was significant at pH 5.8 when compared to pH 1.2 and 7.4. Loading both drugs into the hydrogel resulted in a reduced amount of individual drug release. The significant drug release at acidic pH indicates the potential of the hydrogel for targeted tumor drug delivery.

Korsmeyer–Peppas, Hixson–Crowell, zero-order and Higuchi drug release models were employed in order to evaluate the mechanisms of drug release from the hydrogels (Fig. 2). Korsmeyer–Peppas release model allows the release kinetics to be determined by the diffusion exponent value ( $n$ ). If  $n = 0.5$ , it indicates Fickian diffusion or the drug release is diffusion-controlled as in the Higuchi model. If the diffusion exponent is  $0.5 < n < 1$ , it indicates anomalous diffusion or the drug release is a combination of diffusion-controlled and erosion-controlled. If  $n = 1$ , it indicates a case II transport or drug release that is zero order, in which the release rate is constant and controlled by polymer relaxation. When  $n > 1$ , it indicates super case II transport or the drug release is erosion-controlled [33]. The diffusion exponent for DOX from the hydrogel loaded with only DOX was 0.82, 1.00 and 0.9 at pH 1.2, 5.8 and 7.4, respectively, indicating that the release of DOX was anomalous at pH 1.2, 7.4 and a case II transport at pH 5.8 (Table 3). The diffusion exponent for curcumin from the hydrogel loaded with only curcumin was 1.00, 1.34 and 0.93 at pH 1.2, 5.8 and 7.4, respectively, indicating that the release of DOX was a case II at pH 1.2, a super case II at pH 5.8 and anomalous at pH 7.4. Combining both drugs affected the release mechanism of the drugs. The release of curcumin from hydrogel loaded with both drugs was super case II at pH 1.2, 5.8 and 7.4. However, the release DOX was a super case II at pH 7.4 and anomalous at pH 1.2 and 5.8 (Table 3). The ( $R^2$ ) values are shown in Table 3, which indicate linearity.

**Table 2** Percentage cumulative drug release data over a period of 72 h

Drugs	pH 1.2	pH 5.8	pH 7.4
Doxorubicin	79	68	62
Curcumin	42	91	72
Doxorubicin from DoxCur	65	57	50
Curcumin from DoxCur	34	83	67

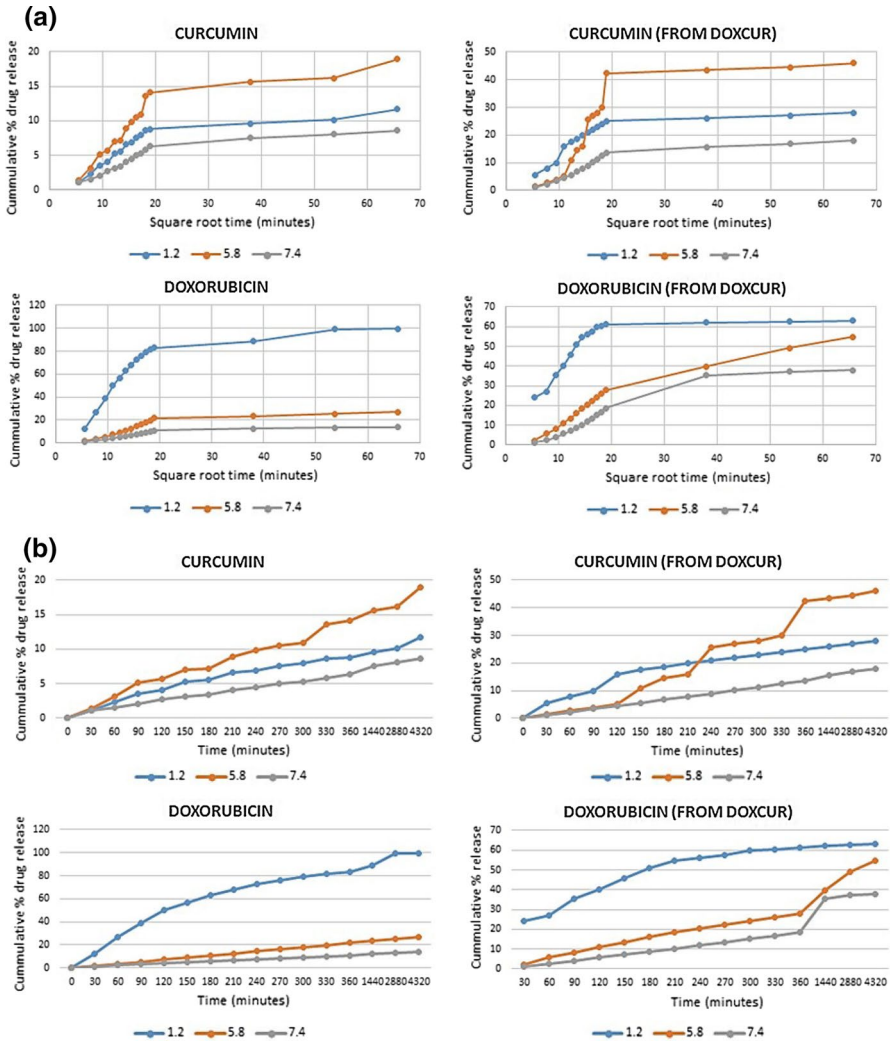


**Fig. 2** a Drug release graphs of Higuchi. b Drug release graphs of zero order. c Drug release graphs of Hixson–Crowell. d Drug release graphs of Korsmeyer–Peppas

## Characterization

### FTIR

The relevant characteristic peaks of the hydrogel (loaded and unloaded with drugs) were revealed by the FTIR spectra obtained. Inferences made from the observed peaks are shown in Fig. 3a, b. The important peaks that were visible in the hydrogels are shown in Table 4. These characteristic peaks for curcumin and DOX are similar to those reported by Pawar et al. [34] and Maheskkuma

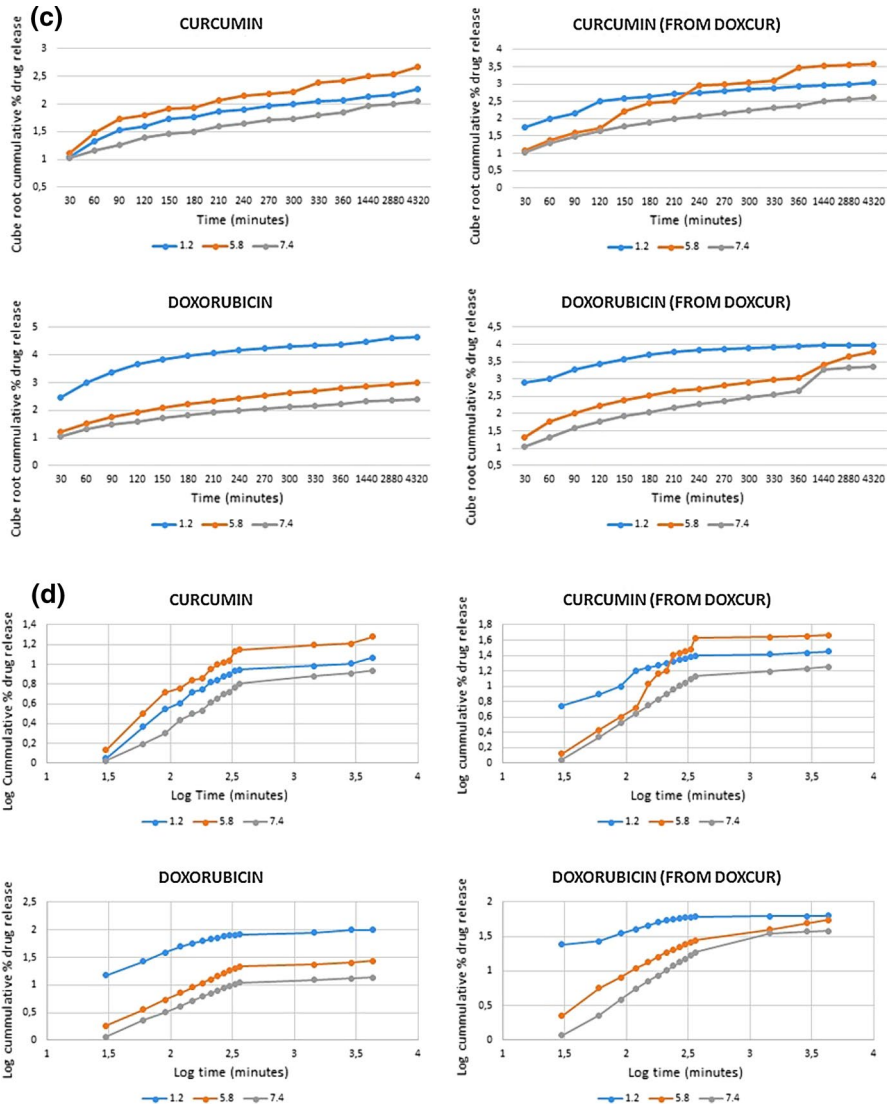


Fig. 2 (continued)

et al. [35], respectively. Hydrogel loaded with curcumin exhibited peaks at 2980, 1600–1500, 1615 and 1100  $\text{cm}^{-1}$ , respectively, for C–H stretching, C=C aromatic and C–O stretching, respectively. Hydrogel loaded with DOX.HCl showed significant absorption peaks at 3300, 1729, 1600–1500 and 1010  $\text{cm}^{-1}$ , respectively. FTIR spectrum for the hydrogel loaded with both drugs revealed characteristic peaks at 3300, 1720, 1600–1500 and 1010  $\text{cm}^{-1}$ , confirming the successful loading of both drugs into the hydrogels (Fig. 3).

**Table 3** Drug release data for (a) Higuchi and zero-order release models, (b) Hixson–Crowell’s and Korsmeyer–Peppas release models

Drugs	Higuchi model			Zero-order model										
	pH 1.2	pH 5.8	pH 7.4	pH 1.2	pH 5.8	pH 7.4								
	$R^2$	$k$	$R^2$	$R^2$	$k$	$R^2$								
<b>(a) Higuchi and zero-order release models</b>														
Doxorubicin	0.98	11.84	0.98	8.35	3.60	0.97	3.01	0.97	0.001	0.96	0.58			
Curcumin	0.99	2.12	0.98	3.94	1.55	0.97	1.09	0.96	1.139	0.95	0.66			
Doxorubicin from DoxCur	0.98	5.73	0.99	9.59	5.51	0.95	19.47	0.97	1.375	0.96	0.80			
Curcumin from DoxCur	0.98	2.48	0.99	2.71	5.32	0.96	3.34	0.95	0.026	0.97	0.09			
Drugs	Hixson–Crowell’s model			Korsmeyer–Peppas model										
	pH 1.2	pH 5.8	pH 7.4	pH 1.2	pH 5.8	pH 7.4								
	$R^2$	$k$	$R^2$	$n$	$R^2$	$n$								
<b>(b) Hixson–Crowell’s and Korsmeyer–Peppas release models</b>														
Dox	0.98	2.12	0.98	1.07	0.85	0.82	0.98	1.22	1.00	0.99	1.22	0.90	0.99	1.25
Cur	0.98	0.90	0.99	0.81	0.99	1.00	0.99	1.10	1.34	0.98	1.78	0.95	0.99	1.09
Dox from DoxCur	0.98	2.75	0.98	0.99	0.98	0.91	0.98	1.73	0.98	0.99	1.03	1.13	0.99	1.62
Cur from DoxCur	0.99	1.58	0.98	0.86	0.98	1.21	0.98	2.19	1.45	0.98	2.13	1.01	0.99	1.46

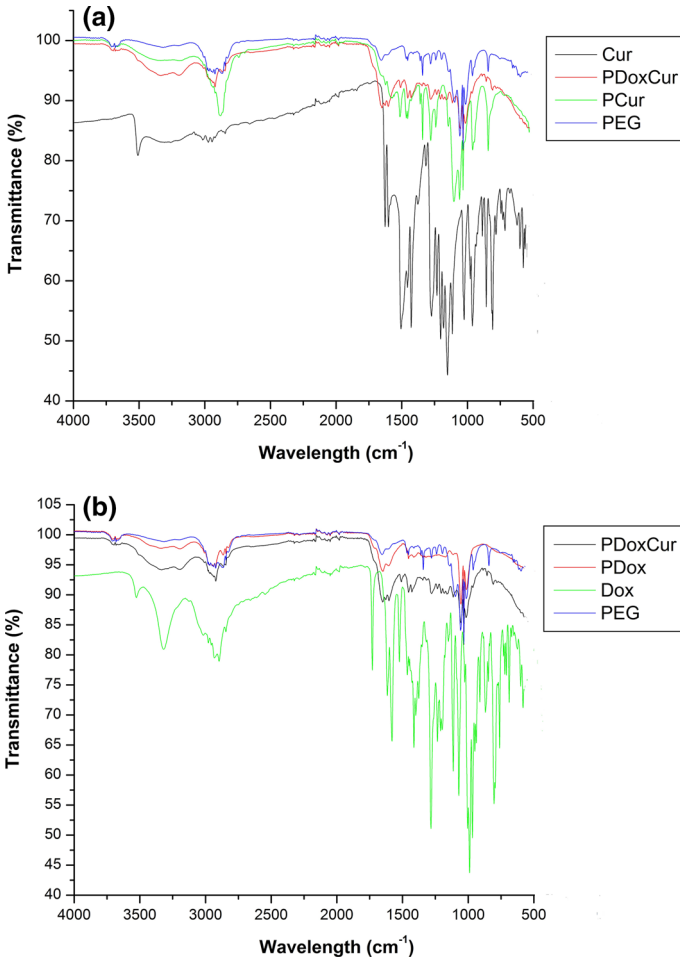


Fig. 3 a, b FTIR spectra of the hydrogels

### XRD

The changes in the morphological structure and crystallinity that occurred before and after loading the hydrogel with the drug(s) were studied using XRD. Figure 4a, b shows the significant changes in the diffraction pattern of the hydrogel loaded with drug(s). The drugs showed characteristic crystalline peaks. Curcumin showed major reflections, corresponding to Bragg’s angle  $2\theta$  at  $8^\circ$ ,  $9^\circ$ ,  $12^\circ$ ,  $15^\circ$ – $19.5^\circ$ ,  $21^\circ$  and  $24^\circ$ – $29^\circ$ , respectively, but strongest at  $9^\circ$  and  $18^\circ$ . Doxorubicin revealed major reflections corresponding to Bragg’s angle at  $4^\circ$ ,  $8^\circ$ ,  $10^\circ$ ,  $11^\circ$ ,  $13.5^\circ$ ,  $15^\circ$ ,  $17^\circ$ ,  $18^\circ$ ,  $19.5^\circ$ ,  $21^\circ$ ,  $24^\circ$ ,  $25^\circ$ ,  $26^\circ$ ,  $30.5^\circ$ ,  $31^\circ$ ,  $33.5^\circ$ ,  $34.5^\circ$ ,  $35.5^\circ$  and  $36.5^\circ$ , respectively, but strongest at  $4^\circ$ ,  $17^\circ$ ,  $18^\circ$ ,  $19.5^\circ$  and  $21^\circ$ , respectively. Broad peaks were seen at  $12^\circ$ – $28^\circ$ ,  $12^\circ$ – $19^\circ$ ,  $22^\circ$ – $25^\circ$  and  $13^\circ$ – $28^\circ$  for PDoxCur, PDox and PCur, respectively.

**Table 4** FTIR absorption peaks

Frequency (cm <sup>-1</sup> )	Indication (type of bond)	Inference
<b>Doxorubicin</b>		
3357–3560	O–H	Hydroxyl stretching
2750–2980	N–H and O–H	Amine and hydroxyl stretching
1730	C=O	Ketone stretching
1309	C–O–C	Ether stretching
1120	C–O	Tertiary alcohol
1000	C–O	Secondary alcohol
590–899	C–O	Primary alcohol
<b>Curcumin</b>		
3500	O–H	Hydroxyl stretching
2938	C–H	Alkane stretching
1590–1615	C=O	Ketone stretching
1500–1400	C=C	Aromatic stretching
1402	C–O	Phenol stretching
1205–1290	C–O	Ethanol stretching
650–960	C–H	Benzoate trans-C–H vibration
<b>PEG</b>		
3300–3600	O–H	Hydroxyl stretching
2980–3000	C–H	Alkane stretching
1700–1600	C=O	Amide stretching
1392–1506	C–H	Alkane scissoring/bending
972–1050	C–O	Alcohol stretching
435–560	C–C	Vibration

## SEM

An irregular topography of the surface of PEG, curcumin and doxorubicin is shown in Fig. 5. These images are comparable to those obtained by Jayakumar et al. [36] and Rachmawati et al. [37]. The PEG-based hydrogel appeared coarse and irregular in shape, while curcumin exhibited block-shaped morphology and doxorubicin was spherical in shape. However, there was a change in the morphology of the hydrogel loaded with drug(s) (PDox, PCur and PDoxCur). These changes as shown in Fig. 5 are the result of the incorporation and absorption of the drugs by the polymer matrix of the hydrogel. The morphology of the hydrogel loaded with curcumin (PCur) was a combination of fibrous and irregular morphology. The hydrogel loaded with DOX (PDox) displayed swollen topology and folded morphology. Loading both drugs into the hydrogels resulted in hydrogels with a combination of folded morphology, swollen topology with a compact structure.



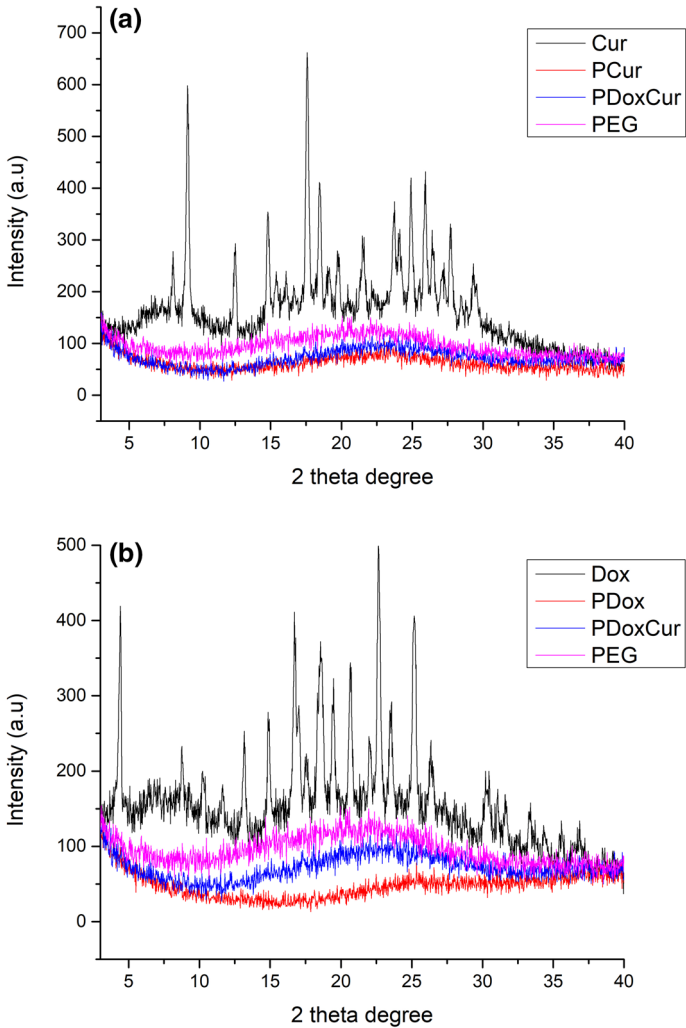
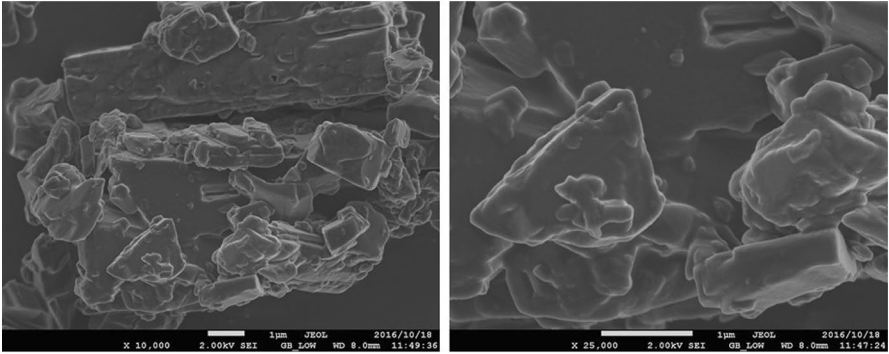
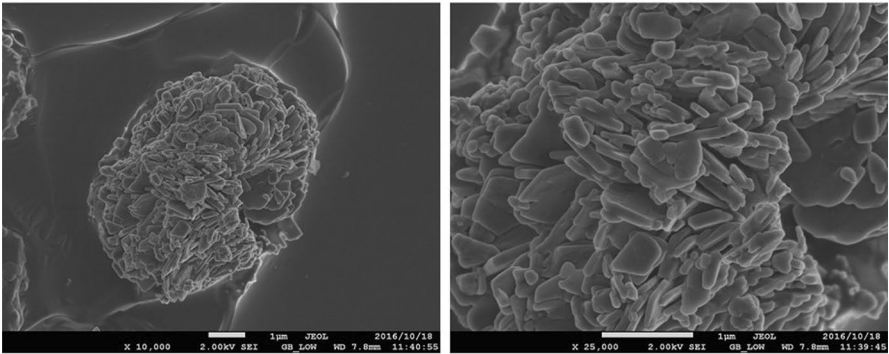
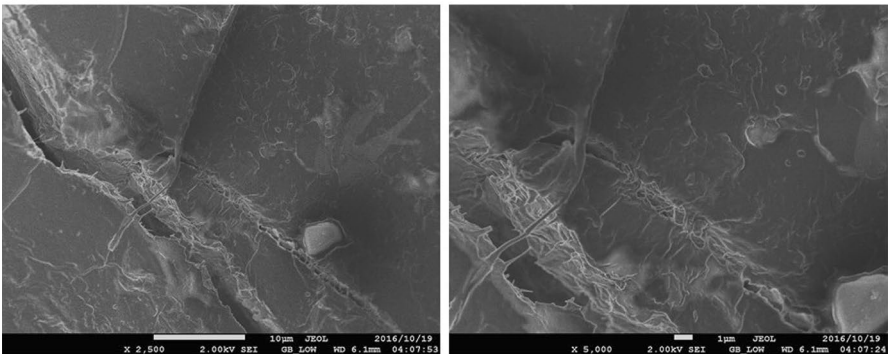


Fig. 4 a, b XRD graphs

**TGA**

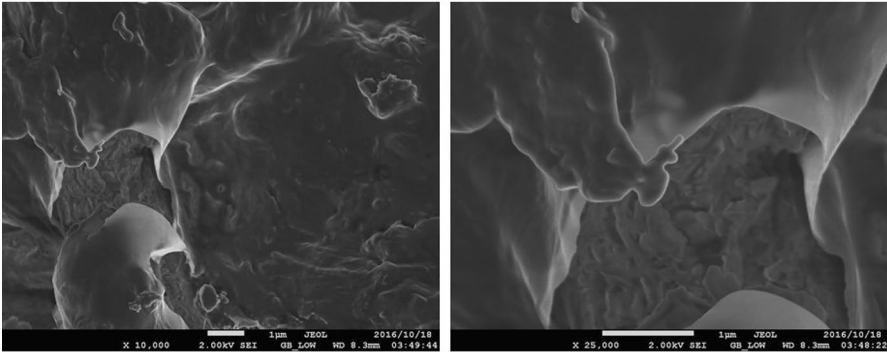
Thermal analysis was carried out in order to study the thermal behavior of the drug(s) and hydrogel loaded with the drugs. Figure 6 shows the various degradation steps of the hydrogels and drugs. It was observed that the TGA curve of the drugs had multiple degradation steps, while the neat hydrogel had a single step. An initial weight loss as a result of the removal of water was observed in all samples at different temperatures. The % initial weight loss in the hydrogel loaded with curcumin was 9% at 202 °C followed by weight loss of 37% and 79% at 360 °C and 564 °C, respectively. The % weight loss in the hydrogel loaded with

**(a)****(b)****(c)**

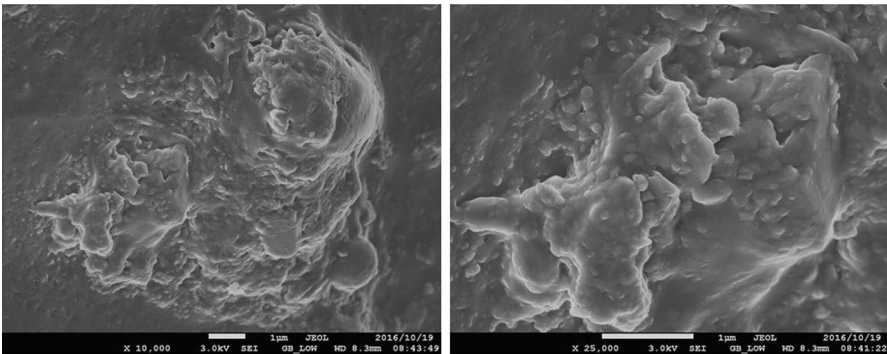
**Fig. 5** **a** SEM images of curcumin, **b** SEM images of doxorubicin, **c** SEM images of PEG-curcumin, **d** SEM images of PEG-doxorubicin, **e** SEM images of PEG-doxorubicin-curcumin, **f** SEM images of PEG

DOX was characterized by an initial weight loss of 7% at 200 °C followed by a second and third weight loss of 38% and 77% at 372 °C and 557 °C, respectively. The hydrogel loaded with both drugs exhibited a weight loss of 11% at 222 °C,

(d)



(e)



(f)

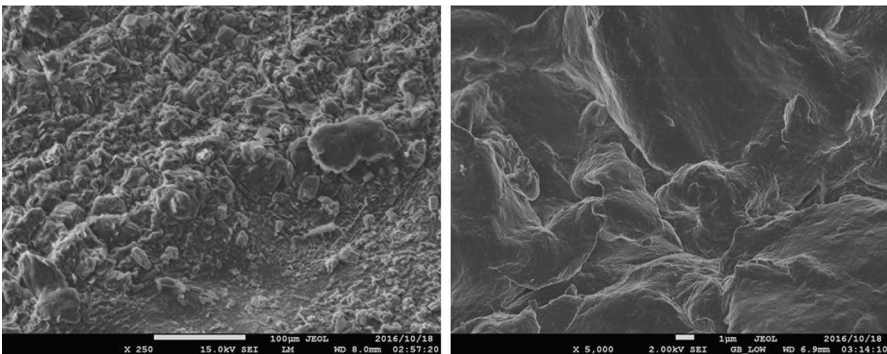


Fig. 5 (continued)

34% at 351 °C and 73% at 537 °C, respectively. The drug exhibited weight loss of 4% at 239 °C for curcumin, followed by weight loss of 54 and 98% at 422 °C and 547 °C, respectively. Dox weight loss was 3% at 204 °C, 49% at 518 °C and 99% at 617 °C. The hydrogel without the drug exhibited 3% weight loss at 212 °C and 90% weight loss at 418 °C.

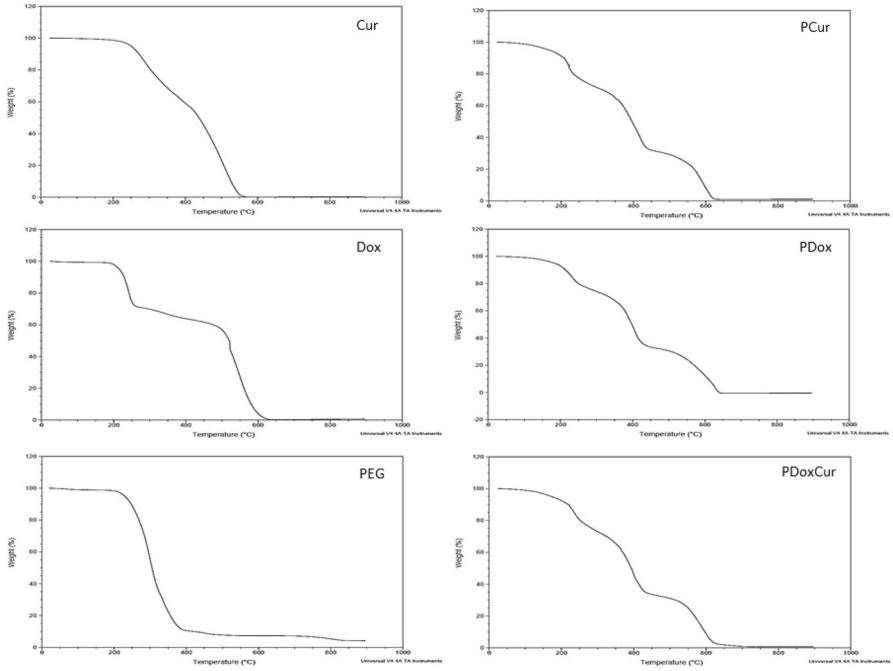


Fig. 6 TGA graphs

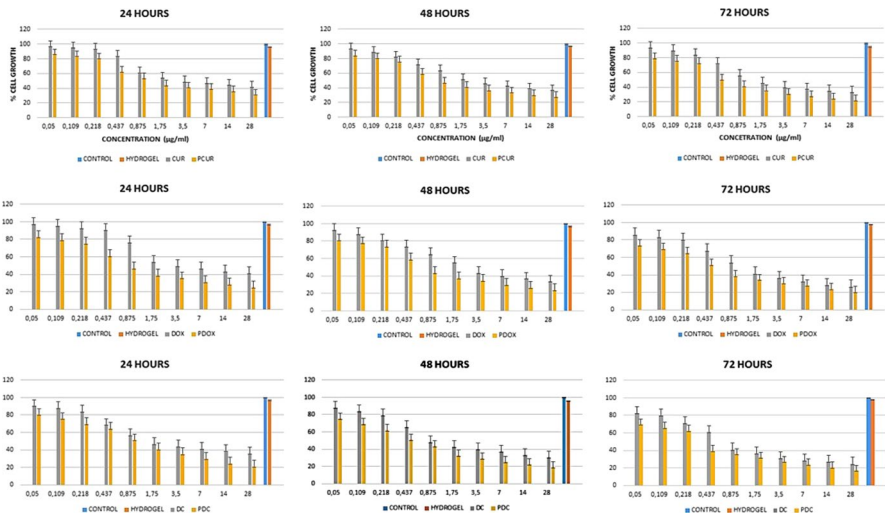


Fig. 7 Cell viability graphs

## In vitro cytotoxicity studies

The cytotoxic and anticancer properties of doxorubicin and curcumin on MCF-7 cells were evaluated (Fig. 7). These were achieved by treating MCF-7 cell lines with hydrogel loaded with the individual drugs independently as well as in combination. Results demonstrated that the incorporation of these drugs showed a greater efficacy compared to the free drugs (unloaded drugs). However, in 24 h, the hydrogel loaded with both drugs did not show a significant decrease in cell viability when compared to other groups. However, as shown in Fig. 7, at 72 h, there was a significant reduction ( $p < 0.05$ ) of viability in the groups exposed to hydrogel drug(s). The cell viability effects of the hydrogel loaded with the drug were time- and dose-dependent, suggesting that the amount of drug needed to reduce the cell viability was released from the hydrogel between 48 and 72 h. Increasing the amount of drug loaded into the hydrogels also significantly reduced the cell viability. The % cell viability of the hydrogel without the drug was 98%, which further revealed the non-toxic nature of the hydrogel. Loading DOX and curcumin into the hydrogel resulted in significant cell viability with decreased  $IC_{50}$  from 0.93 to 0.30  $\mu\text{g/mL}$  over a period of 72 h, revealing the synergistic inhibitory effect of doxorubicin and curcumin on the cell growth of breast cancer cells (Table 5). At a concentration of 28  $\mu\text{g/mL}$ , the cell viability decreased significantly.

## Discussion

The swelling capacity of the hydrogel was pH-dependent, and it was characterized by reduced swelling at acidic pH of 1.2 and 5.8, as well as enhanced swelling at the pH 7.4 (Fig. 1a, b). The low swelling capacity of the hydrogel at acidic pH is attributed to the COOH groups present in the network, which remained non-ionized at acidic pH. The strong hydrogen bonding interactions between carboxylic groups of acrylic acid and hydroxyl groups of gum acacia and PEG resulted in a network that did not permit a significant amount of movement of polymeric segments within the hydrogel, thereby hindering the water uptake. However, at pH 7.4, there was ionization of  $-\text{COOH}$  groups, resulting from repulsion of similarly charged  $-\text{COO}^-$  groups in the macromolecular chains. The ionization also resulted in an increase in ion osmotic pressure. Similar findings were reported by other researchers [38–41]. The swelling capacity of the hydrogel was also influenced by the temperature. At 37  $^{\circ}\text{C}$ , the swelling of the hydrogel was significant compared to its swelling at

**Table 5**  $IC_{50}$  data of the hydrogels

Incubation time (h)	$IC_{50}$ values ( $\mu\text{g/mL}$ )					
	Cur	PCur	Dox	PDox	DoxCur	PDoxCur
24	0.72	0.51	1.00	0.64	0.59	0.93
48	0.68	0.48	0.80	0.50	0.53	0.42
72	0.60	0.41	0.74	0.47	0.50	0.31

room temperature (Fig. 1b). At a higher temperature, there is a reduced interaction between the polymer chains, thereby allowing more water uptake into the matrix of the gel. The destruction of hydrogen bonding between polymer molecules at a higher temperature increased the chain mobility, thereby facilitating the network expansion. Several researchers reported similar findings in which hydrogel water uptake was enhanced at a higher temperature, revealing their potential application as drug delivery system [42–44]. High temperature also increased the segmental mobility of the hydrogel chains, thereby generating voids for enhanced penetration of water molecule, resulting in the increased swelling ratio [45]. The diffusion coefficient of the hydrogels at room temperature was highest at pH 7.4 when compared to pH 5.8 and 1.2, suggesting that the matrix network of the hydrogels was more relaxed at pH 7.4 than at pH 1.2, resulting in faster diffusion. At 37 °C, the diffusion coefficient was highest at pH 7.4 and lowest at pH 1.2 and 5.8 (Table 1). Similar findings were reported by some researchers [46, 47]. The swelling mechanism of the hydrogel at room temperature was Fickian at pH 1.2 and non-Fickian (anomalous) in the buffers of pH 5.8 and 7.4. At 37 °C, the swelling mechanism of the hydrogel was pseudo-Fickian at pH 1.2, 5.8 and anomalous at pH 7.4.

The entrapment efficiency of the drug into the hydrogel was over 90%. The release of the DOX.HCl was significant at pH 1.2 when compared to pH 7.4, suggesting that at low pH, the hydrophilicity and solubility of DOX are enhanced by increasing protonated amine groups on DOX, thereby resulting in its enhanced release from the hydrogel (Fig. 2). The electrostatic interactions between amine groups of DOX and carboxylic groups in the hydrogel also attributed to the enhanced release of DOX from the hydrogel at low pH. At pH 7.4, the existence of significant electrostatic attraction between the positively charged molecules of DOX and the negatively charged carboxyl groups hindered the release of DOX from the hydrogel. A similar release profile of DOX was reported by other researchers to be significant at low pH [48–50]. The significant release of DOX at pH 1.2 is useful because reports have shown that the extracellular pH of tumor tissue is significantly lower than the extracellular pH of normal tissue and the intracellular pH of tumor and normal tissues is similar [49, 51]. The low intra-tumoral pH influences how the tumors respond to treatments. Low pH increases the cellular uptake of weak acidic drugs such as cisplatin, thereby increasing the overall therapeutic effect of the drugs, while low pH reduces the uptake of weakly basic drug and reduce their effects such as DOX [49, 51, 52].

The release of curcumin at pH of 5.8 was enhanced when compared to pH 1.2 and 7.4 (Fig. 2). This finding revealed that curcumin can be released at the tumor cells because the pH value of the tumor cells is lower than the pH of the normal tissue. A similar observation was reported by Zeighamian et al. [53]. However, combining both drugs resulted in a reduced amount of individual drug release. The amount of curcumin and DOX released was enhanced at pH 1.2 and 5.8, respectively. This finding further revealed that this system is suitable for the release of drugs to the tumor cells. A similar finding was reported by other researchers [54, 55]. From the drug release models shown in Table 2, the release mechanism of the drugs from the hydrogel was a combination of diffusion-controlled, erosion-controlled, polymer relaxation-controlled and pH-dependent, respectively.

FTIR spectrum of the hydrogel loaded with both drugs revealed characteristic peaks at 3300, 1720, 1600–1500 and 1010  $\text{cm}^{-1}$ , confirming the successful loading of the drugs into the hydrogels (Fig. 3a, b). These peaks suggested the absence of interaction between the drug and the hydrogel network. The XRD diffraction pattern of the hydrogel was characterized by broad peaks, indicating the amorphous nature of the hydrogels. This result is similar to the report obtained by Qiao et al. [56]. The XRD pattern of the hydrogel loaded with drug(s) (PDox, PCur and PDox-Cur) showed that the crystalline peaks of the drug(s) disappeared, thus confirming the incorporation of the drug(s) (Fig. 4a, b). This can be compared to the report by Anitha et al. [57]. However, broad peaks were visible at  $12^{\circ}$ – $28^{\circ}$ ,  $12^{\circ}$ – $19^{\circ}$ ,  $22^{\circ}$ – $25^{\circ}$  and  $13^{\circ}$ – $28^{\circ}$  for PDoxCur, PDox and PCur, respectively [58, 59]. Furthermore, the intensity of the peaks for both drugs was decreased in the hydrogel loaded with the drug(s). Also, there was no crystallinity observed in the hydrogel loaded with drug(s) resulting from the dispersion of the drug at the molecular level of the polymer matrix. Similar observations were reported by Chavis et al. [60]. Generally, it is necessary for the hydrogel to have less structural stability for ease of degradation. The low crystallinity of the hydrogel indicates less structural stability of the hydrogels.

The morphology of the hydrogel loaded with both drugs was compact, suggesting a strong aggregation of the hydrogel and drug(s) via non-covalent forces mediated by the drug(s) (Fig. 5). This was similarly reported by She et al. [61]. Hydrogel loaded with a single drug was characterized by fibrous and irregular morphology for curcumin and swollen topology with folded morphology for DOX. The morphology of the PEG hydrogel was irregular and coarse. A similar finding was reported by Xu et al. [62]. Furthermore, the thermal stability of the drug was improved when incorporated into the carriers (Fig. 6). A similar finding was reported by Thakur et al. [63]. The moisture content of the hydrogel was low in the range of 7–11%, which is acceptable, indicating the good stability of the hydrogel on storage.

The cell viability effects of the hydrogel loaded with the drug were time- and dose-dependent (Fig. 7). Reduced cell viability was significant between 48 and 72 h, which confirmed that the amount of drug release between 48 and 72 h was high when compared to 24 h. The cell viability effect of the drug-loaded hydrogel was significant in hydrogel loaded with a high amount of drug. The hydrogel without the drug revealed cell viability effects which were not significant, indicating the non-toxic nature of the hydrogels. Similar findings were reported by some researchers in which the % cell viability effects from drug-loaded hydrogels were time- and dose-dependent [64–66]. These observations are similar to that which were reported by Barui et al. [27]. In the report by Zhang et al. [29], the conjugation of DOX and curcumin into nanoparticles did not result in any enhanced synergistic effects because of quick internalization and removal of free DOX and Cur through passive diffusion by cancer cells, resulting in short antitumor effects of the formulation. Curcumin is reported to be a modulator that can enhance DOX-induced antitumor activity and also reduce adverse effects by suppressing lipid peroxidation in normal tissue. Curcumin enhances DOX antitumor activity via main caspase-independent cell death [67, 68]. These results suggest that PEG-based hydrogel is a potential system for the delivery of anticancer drugs for the treatment of breast cancer. The good features of

the hydrogel suggest that it is a potential delivery system for enhanced efficacy of drugs with poor bioavailability, for targeted delivery and for combination therapy.

## Conclusion

PEG-based hydrogel was prepared via free radical polymerization followed by loading of curcumin and DOX into the hydrogel. The hydrogel was characterized using different characterization techniques, and the results showed that the drugs were successfully incorporated into the hydrogel. The study showed that the release of individual drug from the hydrogel loaded with both drugs was influenced by the interaction of the drugs. The *in vitro* cytotoxicity assay further confirmed an enhanced anticancer effect of the drug(s)-loaded hydrogel on treated cell lines when compared to the free drugs. This suggests that the PEG-based hydrogel has the potential to serve as a drug delivery vehicle for anticancer drugs. However, it is advised that further *in vivo* studies be carried out.

**Acknowledgements** The financial supports from the National Research Foundation (NRF), the South Africa Medical Research Council (Self-Initiated Research) (MRC) and the North-West University (NWU), South Africa, toward this research are hereby acknowledged. The views and opinions expressed in this manuscript are those of the authors and not of NWU, MRC or NRF.

## Compliance with ethical standards

**Conflict of interest** The authors report no conflicts of interest.

## References

1. Torre LA, Bray F, Siegel RL et al (2015) Global cancer statistics. *CA Cancer J Clin* 65:87–108
2. Mondal J, Panigrahi AK, Khuda-Bukhsh AR (2014) Conventional chemotherapy: problems and scope for combined therapies with certain herbal products and dietary supplements. *Austin J Mol Cell Biol* 1(1):1–10
3. Asghar U, Meyer T (2012) Are there opportunities for chemotherapy in the treatment of hepatocellular cancer? *J Hepatol* 56:686–695
4. Greco F, Vicent MJ (2009) Combination therapy: opportunities and challenges for polymer–drug conjugates as anticancer nanomedicines. *Adv Drug Deliv Rev* 61:1203–1213
5. Saraswathy M, Gong S (2013) Different strategies to overcome multidrug resistance in cancer. *Bio-technol Adv* 31:1397–1407
6. Deepa K, Singha S, Panda T (2014) Doxorubicin nanoconjugates. *J Nanosci Nanotechnol* 14:892–904
7. Wilken R, Veena MS, Wang MB et al (2011) Curcumin: a review of anti-cancer properties and therapeutic activity in head and neck squamous cell carcinoma. *Mol Cancer* 10:12–15
8. Misra R, Sahoo SK (2011) Coformulation of doxorubicin and curcumin in poly (D, L-lactide-co-glycolide) nanoparticles suppresses the development of multidrug resistance in K562 cells. *Mol Pharm* 8:852–866
9. Hui-TienLiu Yuan-SoonHo (2018) Anticancer effect of curcumin on breast cancer and stem cells. *Food Sci Hum Wellness* 7:134–137
10. Vallianou NG, Evangelopoulos A, Schizas N, Kazazis C (2015) Potential anticancer properties and mechanisms of action of curcumin. *Anticancer Res* 35:645–651



11. Tuorkey MJ (2014) Curcumin a potent cancer preventive agent: mechanisms of cancer cell killing. *Interv Med Appl Sci* 6:139–146
12. Thorn CF, Oshiro C, Marsh S, Hernandez-Boussard T, McLeod H, Klein TE, Altman RB (2011) Doxorubicin pathways: pharmacodynamics and adverse effects. *Pharmacogenet Genomics* 21:440–446
13. Patel AG, Kaufmann SH (2012) How does doxorubicin work? *ELife* 1:e00387
14. Vashist A, Kaushik A, Vashist A et al (2016) Recent trends on hydrogel based drug delivery systems for infectious diseases. *Biomater Sci* 4:1535–1553
15. Wu J, Zhao X, Wu D et al (2014) Development of a biocompatible and biodegradable hybrid hydrogel platform for sustained release of ionic drugs. *J Mater Chem* 2:6660–6668
16. Sinha MK, Gao J, Stowell CE et al (2015) Synthesis and biocompatibility of a biodegradable and functionalizable thermo-sensitive hydrogel. *Regen Biomater* 2:177–185
17. Wang Y, Chen L, Tan L, Zhao Q, Luo F, Wei Y, Qian Z (2014) PEG–PCL based micelle hydrogels as oral docetaxel delivery systems for breast cancer therapy. *Biomaterials* 35:6972–6985
18. Seib FP, Tsurkan M, Freudenberg U, Kaplan DL, Werner C (2016) Heparin-modified polyethylene glycol microparticle aggregates for focal cancer chemotherapy. *ACS Biomater Sci Eng* 2:2287–2293
19. Li M, Li H, Li X, Zhu H, Xu Z, Liu L, Ma J, Zhang M (2017) A bioinspired alginate-gum Arabic hydrogel with micro-/nanoscale structures for controlled drug release in chronic wound healing. *ACS Appl Mater Interfaces* 9:22160–22175
20. Sarika PR, James NR (2015) Preparation and characterisation of gelatin–gum arabic aldehyde nanogels via inverse miniemulsion technique. *Int Biol Macromol* 76:181–187
21. Giray S, Bal T, Kartal AM et al (2012) Controlled drug delivery through a novel PEG hydrogel encapsulated silica aerogel system. *J Biomed Mater Res A* 100:1307–1315
22. Jiang G, Sun J, Ding F (2014) PEG–g–chitosan thermosensitive hydrogel for implant drug delivery: cytotoxicity, in vivo degradation and drug release. *J Biomater Sci* 25:241–256
23. Singh B, Dhiman A (2017) Evaluation of gentamicin and lidocaine release profile from gum acacia-crosslinked-poly (2-hydroxyethylmethacrylate)-carbopol based hydrogels. *Curr Drug Deliv* 14:981–991
24. Shaikh MM, Lonikar MS, Lonikar SV (2014) Gum acacia-acrylic acid hydrogels: pH sensitive materials for drug delivery system. *Asian J Res Chem* 7:407–411
25. Huang GQ, Cheng LY, Xiao JX et al (2016) Genipin-crosslinked O-carboxymethyl chitosan–gum arabic coacervate as a pH-sensitive delivery system and microstructure characterization. *J Biomater Appl* 31:193–204
26. Cao H, Yang Y, Shao ZZ (2015) Doxorubicin hydrochloride and curcumin loaded silk fibroin/hydroxypropylcellulose hydrogels for localized chemotherapy of cancer. *J Control Release* 213:e8–e152
27. Barui S, Saha S, Mondal G, Haseena S, Chaudhuri A (2014) Simultaneous delivery of doxorubicin and curcumin encapsulated in liposomes of pegylated RGDK-lipopeptide to tumor vasculature. *Biomaterials* 35:1643–1656
28. Zhao X, Chen Q, Li Y, Tang H, Liu W, Yang X (2015) Doxorubicin and curcumin co-delivery by lipid nanoparticles for enhanced treatment of diethylnitrosamine-induced hepatocellular carcinoma in mice. *Eur J Pharm Biopharm* 93:27–36
29. Zhang Y, Yang C, Wang W, Liu J, Liu Q, Huang F, Chu L, Gao H, Li C, Kong D, Liu Q (2016) Co-delivery of doxorubicin and curcumin by pH-sensitive prodrug nanoparticle for combination therapy of cancer. *Sci Rep* 6:21225
30. Varaprasad K, Vimala K, Ravindra S et al (2011) Development of sodium carboxymethyl cellulose-based poly (acrylamide-co-2acrylamido-2-methyl-1-propane sulfonic acid) hydrogels for in vitro drug release studies of ranitidine hydrochloride an anti-ulcer drug. *Polym Plast Technol Eng* 50:1199–1207
31. Varaprasad K, Mohan YM, Ravindra S et al (2010) Hydrogel–silver nanoparticle composites: a new generation of antimicrobials. *J Appl Polym Sci* 115:1199–1207
32. Aderibigbe B, Varaprasad K, Sadiku E et al (2015) Kinetic release studies of nitrogen-containing bisphosphonate from gum acacia crosslinked hydrogels. *Int J Biol Macromol* 73:115–123
33. Holowka EP, Sujata KB (2014) Controlled release system. In: Bellomo EG (ed) *Drug Delivery: materials design and clinical perspective*. Springer, New York
34. Pawar H, Karde M, Mundle N et al (2014) Phytochemical evaluation and curcumin content determination of turmeric rhizomes collected from Bhandara District of Maharashtra (India). *Med Chem* 4:588–591

35. Maheshkuma S, Reddy K, Goud P et al (2013) Formulation and characterization of doxorubicin hydrochloride liposomes by double emulsion method. *Int Res J Pharm* 4:197–201
36. Jayakumar R, Nair A, Rejinold NS et al (2012) Doxorubicin-loaded pH-responsive chitin nanogels for drug delivery to cancer cells. *Carbohydr Polym* 87:2352–2356
37. Rachmawati H, Edityaningrum CA, Mauludin R (2013) Molecular inclusion complex of curcumin- $\beta$ -cyclodextrin nanoparticle to enhance curcumin skin permeability from hydrophilic matrix gel. *AAPS PharmSciTech* 14:1303–1312
38. Shaikh MM, Lonikar MS, Lonikar SV (2014) Gum acacia-acrylic acid hydrogels: pH sensitive materials for drug delivery system. *Asian J Res Chem* 7:407–411
39. Zhang L, Jeong YI, Zheng S et al (2013) Biocompatible and pH-sensitive PEG hydrogels with degradable phosphoester and phosphoamide linkers end-capped with amine for controlled drug delivery. *Polym Chem* 4:1084–1094
40. Garland MJ, Singh TR, Woolfson AD et al (2011) Electrically enhanced solute permeation across poly (ethylene glycol)–crosslinked poly (methyl vinyl ether-co-maleic acid) hydrogels: effect of hydrogel crosslink density and ionic conductivity. *Int J Pharm* 406:91–98
41. Singh TR, Woolfson D, Donnelly R (2010) Solute permeation across poly (ethylene glycol)-crosslinked poly (methyl vinyl ether-co-maleic acid) hydrogels. *J Pharm Pharmacol* 62:829–837
42. Khurma JR, Nand AV (2008) Temperature and pH sensitive hydrogels composed of chitosan and poly (ethylene glycol). *Polym Bull* 59:805–812
43. Gupta NV, Shivakumar HG (2012) Investigation of swelling behavior and mechanical properties of a pH-sensitive superporous hydrogel composite. *Iran J Pharm Res IJPR* 11:481
44. Zhao Y, Su H, Fang L et al (2005) Superabsorbent hydrogels from poly (aspartic acid) with salt-, temperature- and pH-responsiveness properties. *Polymer* 46:5368–5376
45. Yin OS, Ahmad I, Amin MC (2015) Synthesis of chemical cross-linked gelatin hydrogel reinforced with cellulose nanocrystals (CNC). In: AIP conference proceedings, Bandung, Indonesia, pp 375–380
46. Bajpai SK, Singh S (2006) Analysis of swelling behavior of poly (methacrylamide-co-methacrylic acid) hydrogels and effect of synthesis conditions on water uptake. *React Funct Polym* 66:431–440
47. Kipcak AS, Ismail O, Doymaz I et al (2014) Modeling and investigation of the swelling kinetics of acrylamide-sodium acrylate hydrogel. *J Chem*. <https://doi.org/10.1155/2014/281063>
48. Hu X, Wei W, Qi X et al (2015) Preparation and characterization of a novel pH-sensitive Salecan-g-poly (acrylic acid) hydrogel for controlled release of doxorubicin. *J Mater Chem B* 3:2685–2697
49. Dadsetan M, Taylor KE, Yong C et al (2013) Controlled release of doxorubicin from pH-responsive microgels. *Acta Biomater* 9:5438–5446
50. Tan SY, Ang CY, Mahmood A et al (2016) Doxorubicin-loaded metal–organic gels for pH and glutathione dual-responsive release. *Chem NanoMat* 2:504–508
51. Gerweck LE, Vijayappa S, Kozin S (2006) Tumor pH controls the in vivo efficacy of weak acid and base chemotherapeutics. *Mol Cancer Ther* 5:1275–1279
52. Ko J, Park K, Kim YS et al (2007) Tumoral acidic extracellular pH targeting of pH-responsive MPEG-poly(beta-amino ester) block copolymer micelles for cancer therapy. *J Control Release* 123:109–115
53. Zeighamian V, Darabi M, Akbarzadeh A et al (2016) PNIPAAm-MAA nanoparticles as delivery vehicles for curcumin against MCF-7 breast cancer cells. *Artifcells Nanomed Biotechnol* 44:735–742
54. Zhang Y, Yang C, Wang W et al (2016) Co-delivery of doxorubicin and curcumin by pH-sensitive prodrug nanoparticle for combination therapy of cancer. *Sci Rep*. <https://doi.org/10.1038/srep21225>
55. Wei L, Cai C, Lin J et al (2009) Dual-drug delivery system based on hydrogel/micelle composites. *Biomaterials* 30:2606–2613
56. Qiao X, Hu F, Hou D et al (2016) PEG assisted hydrothermal synthesis of hierarchical MoS<sub>2</sub> microspheres with excellent adsorption behavior. *Mater Lett* 169:241–245
57. Anitha A, Deepagan V, Rani VD et al (2011) Preparation, characterization, in vitro drug release and biological studies of curcumin loaded dextran sulphate–chitosan nanoparticles. *Carbohydr Polym* 84:1158–1164
58. Shaikh J, Ankola D, Beniwal V et al (2009) Nanoparticle encapsulation improves oral bioavailability of curcumin by at least 9-fold when compared to curcumin administered with piperine as absorption enhancer. *Eur J Pharm Sci* 37:223–230
59. Yallapu MM, Jaggi M, Chauhan SC (2010)  $\beta$ -Cyclodextrin-curcumin self-assembly enhances curcumin delivery in prostate cancer cells. *Colloids Surf B Biointerfaces* 79:113–125

60. Chavis MA, You NH, Maeda R et al (2012) Cleavable self-organized thin films: block copolymers and brushes. Abstracts of Papers of the American Chemical Society, Amer Chem Soc 1155, 16th St, Nw, Washington, DC 20036, USA
61. She W, Luo K, Zhang C et al (2013) The potential of self-assembled, pH-responsive nanoparticles of mPEGylated peptide dendron–doxorubicin conjugates for cancer therapy. *Biomaterials* 34:1613–1623
62. Xu Z, Li J, Zhou H et al (2016) Morphological and swelling behavior of cellulose nanofiber (CNF)/poly (vinyl alcohol)(PVA) hydrogels: poly (ethylene glycol)(PEG) as porogen. *RSC Adv* 6(49):43626–43633
63. Thakur A, Wanchoo R, Singh P (2012) Hydrogels of poly (acrylamide-co-acrylic acid): in vitro study on release of gentamicin sulfate. *Chem Biochem Eng Q* 25:471–482
64. Gil MS, Thambi T, Phan VG et al (2017) Injectable hydrogel-incorporated cancer cell-specific cisplatin releasing nanogels for targeted drug delivery. *J Mater Chem B* 5:7140–7152
65. Quagliariello V, Armenia E, Aurilio C et al (2016) New treatment of medullary and papillary human thyroid cancer: biological effects of hyaluronic acid hydrogel loaded with quercetin alone or in combination to an inhibitor of aurora kinase. *J Cell Physiol* 23:1784–1795
66. Zhang H, Tian Y, Zhu Z et al (2016) Efficient antitumor effect of co-drug-loaded nanoparticles with gelatin hydrogel by local implantation. *Sci Rep* 26:6. <https://doi.org/10.1038/srep26546>
67. Sadzuka Y, Nagamine M, Toyooka T et al (2012) Beneficial effects of curcumin on antitumor activity and adverse reactions of doxorubicin. *Int J Pharm* 432:42–49
68. Mohajeri M, Sahebkar A (2018) Protective effects of curcumin against doxorubicin-induced toxicity and resistance: a review. *Crit Rev Oncol Hematol* 122:30–51